POZNAN UNIVERSITY OF TECHNOLOGY ACADEMIC JOURNALS
No 86 Electrical Engineering 2016

Andrzej KSIĄŻKIEWICZ*

NUMERICAL SIMULATION OF HEAT DISTRIBUTION IN LOW VOLTAGE ELECTRICAL CONTACTS

Electrical contacts are essential part of many electrical appliances, among which are circuit breakers or electromagnetic relays. For their long term usage heat distribution, during normal operation, is a key factor. Heat generated is relative to both the current value and electrical contact resistance. A numerical simulation, using specialized scientific program, is used to observe heat distribution in electrical contacts. This simulation is generated based on real electrical contacts data used in electromagnetic relays.

KEYWORDS: electrical contacts, heat, temperature, simulation, contact material, resistance

1. CONTACT MATERIALS USED IN LOW–VOLTAGE ELECTROMAGNETIC RELAYS

Electric relay is a device designed to produce sudden predetermined changes in one or more electric output circuits, when certain conditions are fulfilled in the electric input circuits controlling the device. An electromechanical relay is a subtype in which the intended response results mainly from the movement of mechanical elements [1]. Relay structural elements are: contacts, dust cover, drive mechanism (solenoid) and the main current paths (Fig. 1). Key part of an electromechanical relay are its electrical contact rivets. They role is to ensure proper electrical connection with little loss of energy and minimal contact resistance. There are many materials than can be used for contacts. These materials are [3]:

- pure materials: copper (*Cu*), silver (*Ag*), gold (*Au*), tungsten (*W*), platinum (*Pt*), palladium (*Pd*) and molybdenum (*Mo*),
- alloys: *AgCdO*, *AgNi*, $AgSnO_2$, *AgPd*, *AgW*, *AuPt*, *AuAg*, *AuNi*, *PtIr*, *PtNi*, *PdCr*, *PdNi*, *CuW*, *AgNiW*, *CuCr*, *Ag*-graphite.

Basic elements used for contacts are copper and silver. Copper is a cheap metal, layer of oxide and sulfide are easily created, requires use of high contact

* Poznan University of Technology.

force. It is used for example in high voltage connectors and oil circuit breakers. Silver is precious metal, sensitive to sulfur and sulfides, quite prone to material transfer. Pure silver contacts can be welded easily. Silver has low melting point; fairly easy for tooling. Silver-plated contacts are used for high frequency circuits. Not suitable for contacts subject to wear. It is not suitable for large currents [4]. Advantages and disadvantages of selected contact materials are presented in Table 1.

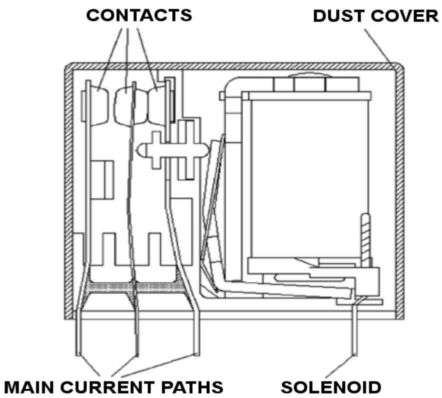

Fig. 1. Relay cross-section [2]

Alloys of AgNi with Ni contents between 10% and 20% are suitable for heavier loads, e.g., for higher currents, as AgNi has a good resistance against contact erosion. The disadvantage is the contact resistance stability and tendency for the welding of nickel [4].

Materials with palladium have a very high chemical resistance against all kinds of erosion. When materials with high palladium content are used, there is a risk of brown powder generation, as previously mentioned. The major advantage is their excellent resistance against material transfer [4].

AgCdO and $AgSnO_2$ alloys are used to switch high loads. Due to their heterogeneity they have unstable contact resistance at low-level switching loads. Resistance values up to 1Ω must be expected [4].

There are few commonly used contact materials for relay rivets. These materials are: AgNi, AgCdO and $AgSnO_2$. Their properties and usage is as follows [2]:

- Silver-nickel alloy (90% Ag-10% Ni) – is most appropriate alloy for switching DC loads, in order to avoid material transfer, it is also wildly used for switching low current non inductive AC loads.
- The compound of silver-cadmium oxide (90% Ag-10% CdO) – has a wide range of applications in power load due to the high welding resistance and arc extinguishing effect. Its field of application is in the range of 12 to 380

VAC and 100 mA to 30A. It is especially used for resistive and inductive loads, such as motors load, heating resistors, lamps and other.

– Silver material + tin oxide (carbon) $AgSnO_2$ – has similar properties to the silver-cadmium oxide, but has a higher thermal stability of the resistance and lower material transferring from one contact to another, which translates into higher stability in DC applications. $AgSnO_2$ contacts also feature a uniform wear and are recommended for applications with loads producing current surges and inductive loads. Some miniature relays offered contain small admixture of indium oxide (In_2O_3). In addition to the good results obtained switching lamps, this material also has excellent behaviour with resistive loads and switching currents up to 16A.

Their selected material properties are presented in Table 1.

Table 1. Silver and Silver Alloys for Low-Level Switching [4]

Contact Material	Advantages	Disadvantages
Ag	High conductivity, 60 MS/m Inexpensive	Formation of Ag sulfides, sticking
AgNi 0.15	High strength	Formation of Ag sulfides, sticking
AgNi 10–20	High erosion protection	Contact welding Material transfer
AgPd 60	High resistance to sulfide formation Good resistance to material transfer	Polymerization
PdRu 10	High conducting reliability	Expensive
$AgCdO/AgSnO_2$	High erosion protection at high current (power circuit breaker)	High and unstable contact resistance in low-level applications

Table 2. Selected properties of contact materials used in low-voltage relays [5]

Material	Density	Melting temperature	Hardness	Thermal conductivity at 20 ºC	Electrical conductivity
	[g/cm^3]	[ºC]	[HB]	[W/(K · m)]	[m/(Ωmm^2)]
AgNi10	10,3	961	50	350	54
AgCdO10	10,2	961	70	307	48
$AgSnO_2$10	9,9	961	70	-	49

Looking at material properties in Table 2 there are little differences between their density and hardness and they have the same melting point temperature. Thermal conductivity has the highest value for AgNi together with the lowest value of electrical conductivity and there is only a small difference between the remaining two materials. These material properties will be used in numerical simulation of heat distribution in contact rivets.

2. CONTACT TEMPERATURE IN STEADY STATE

The flow of electrical current through the conductive elements causes them to heat up. The condition for proper operation of these devices is that the temperature will not reach danger value for the element or its neighbourhood. Continuous current-carrying capacity of the contacts is called the effective value of the current of a constant intensity, which is flowing under certain operating conditions, that results in specified temperature rise to its maximum allowed level. Contacts temperature depends on their shape, material, surface condition, shape of adjacent elements and conditions for heat transfer. Suitable quantitative relationships are determined primarily with respect to single contact point. The course of heating of the current path in the steady state can be determined from the equation [6, 7]:

$$dq + dq_3 = dq_1 \tag{1}$$

where: dq – heat produced in considered wire element in time dt, dq_1 – the heat transfer to the environment from the outside of the element dx in time dt, dq_3 – the amount of heat generated by the element wire length dx in time dt as a result of heat conduction along the element.

The temperature in the area where the contact point is determined as the sum of the following components:

$$\vartheta_p = \vartheta_o + \Delta\vartheta_m' + \Delta\vartheta_m + \Delta\vartheta_p \tag{2}$$

The individual components are expressed by the following formulas:

$$\Delta\vartheta_m' = \frac{k_w \rho_\upsilon}{kAS} I^2 \tag{3}$$

$$\Delta\vartheta_m = \frac{R_{p\upsilon}}{kAS} I^2 \tag{4}$$

$$\Delta\vartheta_m' = \frac{U_p^2}{8\lambda\rho_\upsilon} \tag{5}$$

where*:* S – sectional area of the current path, A – area circuit current path, k_w – current displacement factor, ρ_υ – contact material resistivity at temperature υ*,* k – heat transfer coefficient, λ – coefficient of heat conductivity of the contact material, $R_{p\upsilon}$ – contact resistance at temperature υ, U_p – voltage drop on the contact point, I_p – the current flowing through the contact.

The calculations assume the following values:
$r = 1$, $I = 16$ A, $\upsilon = 40$ ºC, $k_w = 1$, $k = 26{,}44$ $Wm^{-2}K^{-1}$, $\upsilon_o = 30$ ºC, $\alpha = 0{,}004$ K^{-1}
$\rho_\upsilon = 1{,}8 \times 10^{-8}$ Ωm, $\lambda = 350$ $Wm^{-2}K^{-1}$, $R_{p\upsilon} = 0{,}3537$ mΩ

Result of the calculations are presented in Table 3.

Table 3. Result of the calculations of contact point temperature

$\Delta\upsilon_m$' [ºC]	$\Delta\upsilon_m$ [ºC]	$\Delta\upsilon_p$ [ºC]	$\Sigma\Delta\upsilon$ [ºC]
10,24	3,71	0,004	43,95

Particularly interesting is the increase of temperature at the point of contact $\Delta\upsilon_p$. The increase was negligible compared to other calculated values. This leads to the conclusion that the point of contact, under normal conditions, reached almost the same temperature as its immediate neighbourhood. In further stude the $\Delta\upsilon_p$ rise is omitted.

3. COMPUTER SIMULATION OF HEAT DISTRIBUTION IN ELECTRICAL CONTACT

A computer simulation of heat distribution in electrical contact was preformed using a multi-platform application for the solution of physical problems Agros2D, which is based on the Hermes library, developed by the group at the University of West Bohemia in Pilsen. Agros2D is a powerful code for numerical solutions of 2D coupled problems in technical disciplines. Its principal part is a user interface serving for complete preprocessing and postprocessing of the tasks (it contains sophisticated tools for building geometrical models and input of data, generators of meshes, tables of weak forms for the partial differential equations and tools for evaluating results and drawing graphs and maps). The processor is based on the library Hermes2D containing the most advanced numerical algorithms for monolithic and fully adaptive solution of systems of generally nonlinear and nonstationary partial differential equations (PDEs) based on the finite element method of higher order of accuracy. Uses new class of adaptivity algorithms for time-dependent partial differential equations (PDE) that combine adaptive higher-order finite elements (hp-FEM) in space with arbitrary (embedded, higher-order, implicit) Runge–Kutta methods in time [8, 9].

For the simulation of heat distribution in electrical contact a Heat Transfer part of the program was used. Steady state of thermal effects was described using equation 6. Model representing contact rivet is shown on Figure 2. The model was axisymmetrical.

$$-\boldsymbol{div}(\lambda \cdot gradT) + \rho c_p (v \cdot gradT) = Q \quad (6)$$

The following assumptions were made for the presented model:

- contact face dose not conduct heat in any way, as it is close to the opposite contact rivet,
- contact rear surface is connected to pure copper current path,
- contact lateral surface is conducting heat through convection and radiation into air,
- contact point is the heat source.

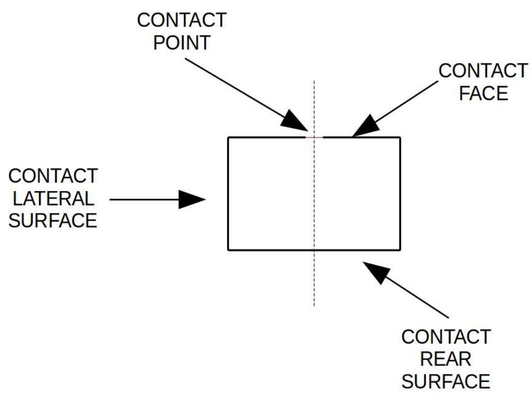

Fig. 2. Contact model used in simulation

Parameters for the contact lateral surface are: surrounding temperature T = 303,15 K (30°C); contact rear surface: α = 425 $Wm^{-2}K^{-1}$; contact point α = 350 $Wm^{-2}K^{-1}$. A key part of the simulation set-up was the calculation of the heat flux for the contact point (Wm^{-2}). It was assumed that heat was generated on the real contact point (spot) surface as presented by Holm [10]. The diameter of contact spot can be calculated as follows:

$$r_p = \sqrt{\frac{F_d}{\pi \alpha HB}} \quad (7)$$

where: F_d – contact force, [N], HB – contact hardness, [-], α – material coefficient, [-].

Contact hardness is a material property, constant for a selected contact material. Contact force is determined by the electromagnetic relay. Material coefficient is determined by contact surface, and typically its value ranges between 0,5 and 0,7. Values used to calculate the contact spot diameter were as follows: F_d = 0,36 N, HB = 70, α = 0,5. The next step was to calculate the heat flux of the contact spot. For this the power generated in the contact was needed. The calculation was made using equation 8. Nominal value of current for the selected relay was taken, I = 16 A. Electrical contact resistance was obtained experimentally, and equal to R_p = 0,9 mΩ. Electrical contact resistance is difficult to calculate analytically and it changes with each contact switching operation [11, 12, 13]. The ½ coefficient is take into account as half of the power generated in contact is turned into heat for one contact rivet and the other half for the second.

$$P_i = \frac{1}{2} I^2 \cdot R_p \qquad (8)$$

where: P_i – power generated in contact, [W], I – effective value of current, [A], R_p – electrical contact resistance, [Ω].

Power generated on the contact surface was calculated using equation 9, with values obtained from equations previously mentioned. This power represents the heat flux that is generated on the contact spot as it would be the only heat source in contact. Heat generated in the rest of contact rivet is not taken into account.

$$P_w = \frac{P_i}{S_p} = \frac{P_i}{\pi r_p^2} \qquad (9)$$

where: P_i – power generated in contact, [W], S_p – contact spot surface, [m^2], P_w – power generated on contact surface [Wm^{-2}].

$AgSnO_2$ was chosen for the simulation as contact material. Thermal steady state was simulated in Argos2D. Results of this simulation (temperature gradient) is shown on Figure 3. Width and height shown where equal to 1mm. Temperature ranges from 30°C, in most part of the contact, to 33,35°C, at contact spot. This temperature rise is dependant only on the heat generated in the contact spot and not in the body of contact rivet. It is clear that this heat affects a small part of the rivet and has immediate impact only for the material in proximity to the contact spot. Figure 4 show magnification of the contact spot. The presented area is 0,2 by 0,2 mm. There are at least two important conclusions here. First is that the temperature near the contact spot has an elliptical gradient with a circular contact spot. This is consistent with Holms [10] theory where the equipotential current lines are elliptical. Second conclusion is that the temperature falls rapidly with growing distance from the contact spot [14, 15]:

$$\tau(x) = \frac{1}{2} I^2 R_z \frac{1}{aS\lambda} e^{-ax} + \tau_p \qquad (10)$$

where: I – nominal current, [A], R – contact resistance, [Ω], λ – thermal conductivity, [$Wm^{-1}K^{-1}$], and a and τ_p are [14]:

$$a = \sqrt{\frac{k_{od} S_{p1}}{\lambda S}} \qquad (11)$$

$$\tau_p = \frac{I^2 \rho}{S} \frac{1}{k_{od} S_{p1}} \qquad (12)$$

where: k_{od} – heat transfer coefficient, [$Wm^{-2}K^{-1}$], S – contact spot cross-section, [m^2], S_{p1} – lateral surface of a dx element of the conductor (in the discussed case is equal to 2πr), [m^2], ρ – contact material electrical resistivity, [Ωm].

Fig. 3. Temperature gradient in contact

For a practical approach two factors can be important:

- high gradient of temperature near the contact spot,
- small temperature rise compared to contact lateral surface.

They can play an important role in determining contact usage through thermography [16]. Through thermography only the lateral surface temperature can be measured. For the electrical contact to work properly the contact spot temperature cannot exceed melting temperature of the material. With the two factors in mind it can be assumed that a proper thermographic temperature reeding of the lateral surface contact temperature ensures proper contact spot temperature.

Figure 5a shows temperature change, on contact face surface (Fig. 2), in function of distance from the contact spot. The distance is limited to 0,2 mm because of negligible temperature change on rest of the surface. The highest temperature can be observed directly in the middle of the contact spot. There can be seen a bend on the beginning of the curve. It is assumed that this bend is associated with the elliptical equipotential current lines, as mentioned before, and that the contact spot is simulated with the radius of 0,01 mm. The temperature falls to around 30°C with the distance reaching just 0,1 mm. That represents 5% of total contact diameter (which is 2 mm). Almost identical temperature change from contact point to rear contact surface can be seen in Figure 5b. The temperature is calculated directly in the axis of the contact. There is no bend on the curve here, and that is the only difference. Temperature falls as rapidly as in previous case.

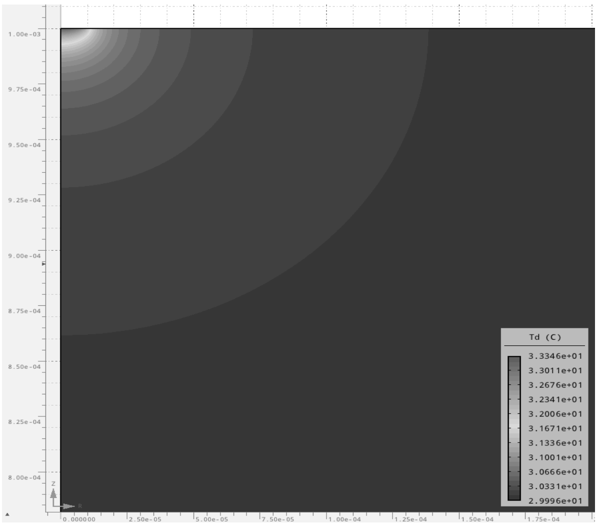

Fig. 4. Temperature gradient in selected part of contact

a) b)

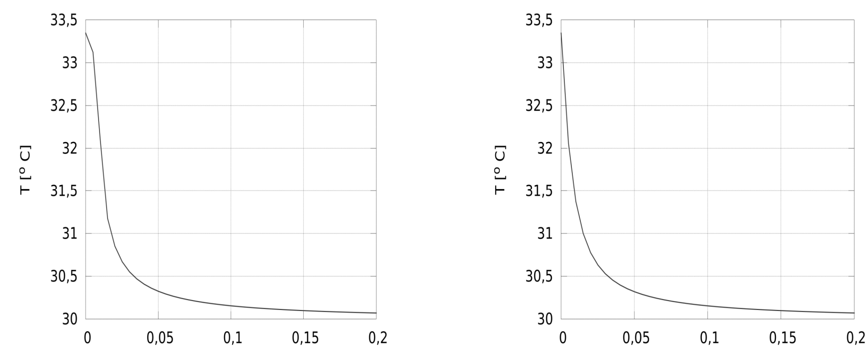

Fig. 5. Temperature change of contact:
a) at contact surface face, b) from contact point to rear contact surface

4. SUMMARY

Maximal working temperature is an important factor for proper electromagnetic relay exploitation. It is determined by many factors, amongst theme are: maximum working current, contact material, contact force, etc. With the usage of numerical software working principle of an electrical device can be investigated. The presented results show that the simulated contact temperature rise is almost the same as the calculated one $\Delta\upsilon_m$. This can lead to a conclusion that the simulation a basic equations produce similar results. The rise of contact spot temperature compared to the lateral surface is around 12%, based on the simulation. Most important outcome of presented work is that, with the usage of thermographics camera, the temperature of contact spot can be determined on satisfactory level. For further studies heat distribution in non steady state are planed. Usage of a program that allows three-dimensional simulation would be a significant improvement.

REFERENCES

[1] International Electrotechnical Vocabulary - part 444: Elementary relays, IEC.

[2] Technical catalogue - Przekaźniki, Relpol S.A., Mar. 2013. (in Polish).

[3] A. Książkiewicz: Comparision of selected contact materials used in low-voltage relays, Poznan University of Technology Academic Journals. Electrical Engineering, 82/2015, s. 207 – 212, Poznań.

[4] M. O. Thurston, Electrical Contacts. Fundamentals, Applications and Technology, Taylor & Francis Group*, LLC,* 2007.

[5] Elesta Elektrotechnik AG, Informacja techniczna, 2002 (in Polish).

[6] H. Markiewicz, Urządzenia elektroenergetyczne, 2006 (in Polish).

[7] S. Kulas, Tory prądowe i układy zestykowe, Oficyna Wydawnicza Politechniki Warszawskiej, 2008 (in Polish).

[8] Karban, P., Mach, F., Kůs, P., Pánek, D., Doležel, I.: Numerical solution of coupled problems using code Agros2D, Computing, 2013, Volume 95, Issue 1 Supplement, pp 381-408.

[9] Solin, P., Korous, L.: Adaptive higher-order finite element methods for transient PDE problems based on embedded higher-order implicit Runge–Kutta methods, Journal of Computational Physics, 2012, Volume 231, Issue 4, pp 1635–1649.

[10] Holm R., Electric Contacts, Springer-Verlag Berlin Heidelberg GmbH, 1981.

[11] J. Janiszewski, A. Książkiewicz, Vacuum switches contact resistance, Computer Applications In Electrical Engineering, vol. 12, pp. 227-236, 2014.

[12] Książkiewicz A., Janiszewski J. Low voltage relay contact resistance change influence by short-circuit current, Eksploatacja i Niezawodnosc – Maintenance and Reliability, 2015, 17 (4): 600–603, http://dx.doi.org/10.17531/ein.2015.4.1.

[13] J. Janiszewski, A. Książkiewicz: Badania modelowe rezystancji zestykowej łączników próżniowych, Poznan University of Technology Academic Journals. Electrical Engineering, 78/2014, s. 167 – 174, Poznań.

[14] Markiewicz H., Urządzenia elektroenergetyczne, WNT, Warszawa, 2006 (in Polish).
[15] A. Książkiewicz, R. Batura: Thermal and electrodynamic characteristics of electrical contacts in steady state, Poznan University of Technology Academic Journals. Electrical Engineering, 74/2013, s. 137 – 142, Poznań.
[16] Kuczyński K., Dymny G., Zastosowanie biernej termografii do kontroli elementów sieci elektroenergetycznych, elektro.info, 9/2015.

(Received: 3. 02. 2016, revised: 3. 03. 2016)